

NATURAL CONVECTION HEAT TRANSFER IN AN INCLINED ANNULAR POROUS MEDIUM

انتقال الحرارة بالحمل الطبيعي في وسط مسامي حلقي مائل

M. S. El Katy, F. F. Araid, E. A. El Negiry, and G. B. Abd El Aziz
Mechanical Power Engineering Department
Mansoura University, Egypt

خلاصة

حذب موضوع انتقال الحرارة في الاوساط المسامية انتباه الباحثين في الآونة الأخيرة نظرا لتزايد التطبيقات الهندسية والتكنولوجية في هذا المجال مثل عمليات استخلاص البترول والصناعات الكيميائية وعمليات العزل الحراري وزيادة الطاقة الحرارية في المجمعات الشمسية، التخلص من النفايات النووية وفي تبريد وعزل المفاعلات النووية وفي تبريد الكابلات الكهربائية.

يقدم هذا البحث دراسة لانتقال الحرارة بالحمل الحر خلال وسط مسامي حلقي مائل ذو نسبة بعديّة ٤١ ونسبة انقطر الخارجي الي القطر الداخلي ٢٠١٤٣. تكون الوسط من اسطوانتين مركزيتين يمثل الفراغ المحصور بينهما وسطا حلقيًا باقطار ٤٥/٢١ مم وطول ٤٩٢ مم معرض لفيض حراري ثابت عند السطح الداخلي بينما يحفظ السطح الخارجي عند درجة حرارة ثابتة، ملئ الوسط للحلقى بكرات من العسلب بقطر ٦,٣ مم ذات بفاذية = ٠,٤٥. الهدف الرئيسي هو ايجاد تأثير زاوية ميل الوسط على انتقال الحرارة ممثلا في درجات الحرارة وعدد نوسيلت، حيث تغيرت زاوية الميل من الوضع الاقنى الى الوضع الرأسي تدريجيا في $0 \leq \theta \leq 90^\circ$ مع تغيير الفيض الحراري من ٤ الى ٣٢٤ وات حيث يتغير رقم رايلى من ١٠ حتى ٥٥٠٠. أظهرت النتائج ان تغير زاوية ميل الوسط للمسامي له تأثيرا كبيرا على خواص انتقال الحرارة، فمع زيادة زاوية الميل تقل كل من درجة الحرارة المتوسطة والتصوي لسطح الفيض الحراري الداخلي كما يزداد كل من عدد نوسيلت المتوسط ومعامل انتقال الحرارة بالحمل الطبيعي. عند رقم رايلى يساوى ٤٠ يبدأ انتقال الحرارة بالحمل الطبيعي، وبزيادة رقم رايلى يزداد كل من عدد نوسيلت المتوسط ومعامل انتقال الحرارة بالحمل. كما تم الحصول على علاقة رياضية تربط رقم نوسيلت المتوسط \bar{Nu} مع كل من زاوية الميل θ ورقم رايلى Rn

ABSTRACT

Experimental study was carried out for the steady laminar natural convection of air in an inclined annulus porous medium, with constant heat flux heated inner cylinder and an isothermally cooled outer cylinder. The primary objective of the study is to show the effect of the inclination angle of the annulus on the local and maximum temperatures of the heated inner cylinder and the local and mean Nusselt number. The geometrical parameters of the annulus are: diameters of 21/45mm, gap width=12mm, length of 492 mm, and an aspect ratio (length/gap width) = 41. The annulus is filled with spherical beads of diameter $d = 6.3$ mm with porosity of 0.45. The operating parameters are: heat flux $4 \leq Q \leq 324$ W, Rayleigh number $10 \leq Ra \leq 550$ and inclination angle $0 \leq \theta \leq 90^\circ$. The results show great influence of the inclination angle on the local and maximum surface temperatures as well as the local and mean Nusselt number. The average Nusselt number is correlated with both the inclination angle θ and the Rayleigh number.

INTRODUCTION

Natural convection heat transfer in enclosures commonly occurs in nature, and engineering and technological applications. This Phenomenon plays an important role in such diverse applications including thermal insulators, storage of solar energy in underground containers, underground cable systems, heat exchangers, food industry, biomedical applications and heat transfer from nuclear fuel rod bundle in nuclear reactors and interior of its canister in either storage or disposal.

There are large number of publications in the literature dealing with natural convection in horizontal and vertical porous annulus. In horizontal porous annulus, Facas and Farouk [1] studied the problem numerically with aspect ratio of 2 and Ra up to 1000. Vasseur et al. [2] presented the same point with uniform internal heat generation for radius ratio $1 \leq R \leq 4$ and $0 \leq Ra \leq 10^4$. Rao et al. [3] and [4] have solved numerically both 2-D and 3-D problems for $R=2$ and $65 < RaDa < 300$. The 2-D bifurcation phenomena have been studied by Himasekhar and Bau [5] for $R=2.5, 2.25,$ and 2.125 . Numerical and experimental study of free convection flows in a horizontal porous annulus was reported by Mojtabi et al. [6] with an aspect ratio=0.5 and $R=2$ using the Christiansen effect to visualize the thermal fields. Mojtabi and M. Mojtabi [7] presented an analytical solution of steady natural convection in a horizontal porous annulus for $R=2.5, 2.25, 2.125$ and 2.0625 and $25 < RaDa < 1000$. A numerical solution of the same 2-D form problem was studied by Barbosa and Saatchian [8] while a numerical simulation of 2-D and 3-D solution was carried out recently by Mojtabi [9] for $R=2$ and 1.414 and an aspect ratio of 2

The first experimental study of natural convection in a vertical porous annulus was presented by Reda [10] who has conducted experiments with constant heat flux on the inner wall for $R=23, A=4.25,$ and $RaDa < 80$ with water-glass combination. Prasad and Kulacki have studied the problem numerically and reported the results for $1 \leq A \leq 20$ and $1 < R \leq 26$ [11], and for $0.3 \leq A \leq 0.9$ and $1 < R \leq 11$ [12], both for $RaDa \leq 10^4$. Another series of experiments on isothermally heated vertical annuli has been reported by Prasad et al. [13] for $R=5.338$ and $A=0.545, 1,$ and 1.46 with various solid-fluid combinations. Natural convection in a vertical porous annulus was performed for constant heat flux on the inner wall experimentally by Prasad et al [14] for $R=3.5$ and 14 and $A=11.08$ and 14.4 and numerically by Prasad [15].

Natural convection in an inclined porous annulus were studied numerically by Fukuda et al. [16], experimentally by Takata et al [17] and analytically with experimental proof by Takata et al [18]. They investigated the 3-D flow configuration with temperature distribution and heat transfer analysis for porosity $\epsilon=0.39,$ $Da=2.51 \times 10^{-6}, A=7.2, R=2,$ and $10 \leq RaDa \leq 300$.

Natural convective heat transfer in an inclined porous annulus has received very little attention. Only one experimental study has been carried out for limited parameters. In the present study, an experimental investigation has been carried out for the free convection in an inclined porous annulus with different inclination angles, $R=2.134, A=41, Pr=0.7, Da=4.583 \times 10^{-4}, \epsilon=0.45,$ and $10 \leq Ra \leq 550$.

EXPERIMENTAL APPARATUS

Schematic layout of the experimental test apparatus is shown in Fig. 1. An annular section (1) which is filled with stainless steel spherical beads of diameter $d=6.3$ mm (2) is portable by means of a pivot (9). The change of inclination angle is achieved by a protractor (10). The inner cylinder (3) is made from copper with length of 540mm and diameters of 13/21 mm, and is heated by an electric heater (4). The outer cylinder (5) which is made of copper with length of 540 and diameters of 45/50 mm is kept approximately at constant temperature by circulating cooling water through a PVC cylinder (6) with diameters 75/70 mm. City water is forced from the bottom tap (7), and leaves at the upper tap (8). The water temperature at the inlet and the outlet of the shell were measured by means of two copper-constantan thermocouples (11). The electric heater (4) has a diameter of 0.5 mm and its effective length is 492mm. The electric heater is covered by electric insulation from porcelain which gives constant heat flux along its effective length. The total electric resistance of the heater equals 100 ohm. The consumed power in the heater is adjusted by a variable voltage auto-transformer (13), voltage regulator (12), and measured by voltmeter (15), ammeter (16) and Wattmeter (14). In order to avoid the heat loss in the longitudinal direction of the annulus, thermal insulation (17) is used at the external two ends of the annulus. The inner cylinder is fixed concentrically inside the outer one by means of teflon pins (18).

The temperatures of the inner and outer surfaces of the annulus were measured by copper-constantan thermocouples (19) of 0.3 mm diameter.

The characteristic parameters in the present study are the local Nusselt number Nu , the mean Nusselt number \bar{Nu} , the Rayleigh number Ra and the Darcy number Da . These parameters are calculated as follows:

$$Nu = q \delta / [k_m (t_i - t_o)], \quad \bar{Nu} = q \delta / [k_m (\bar{t}_i - \bar{t}_o)]$$

$$Ra = g \beta \delta^3 (\bar{t}_i - \bar{t}_o) (\rho c) / v k_m, \quad \text{and} \quad Da = K / \delta^2$$

where \bar{t}_i and \bar{t}_o are the mean temperatures of the inner and outer cylinders respectively, δ is the characteristic length and equals $(r_o - r_i)$, q is the heat flux per unit area, Q is the input power. K is the permeability of the porous medium and equals to $\{d^2 \varepsilon^3 / 180(1 - \varepsilon)^2\}$ [9, 11], d is the bead diameter, ε is the porosity, and h is the overall coefficient of heat transfer at the inner cylinder = $q / (\bar{t}_i - \bar{t}_o)$.

β , ρ , c , and v are the coefficient of thermal expansion, density, specific heat, and the kinematic viscosity of the air at its mean temperature, respectively.

The effective thermal conductivity k_m is determined by applying a low electric power of about 1-4W to the electric heater, where the heat transfer process is contributed only by conduction

RESULTS AND DISCUSSION

Experiments were conducted to study the natural convective heat transfer through an inclined annulus filled with porous medium saturated with air. The main goal of this study is to show the effect of inclination angle on the heat transfer

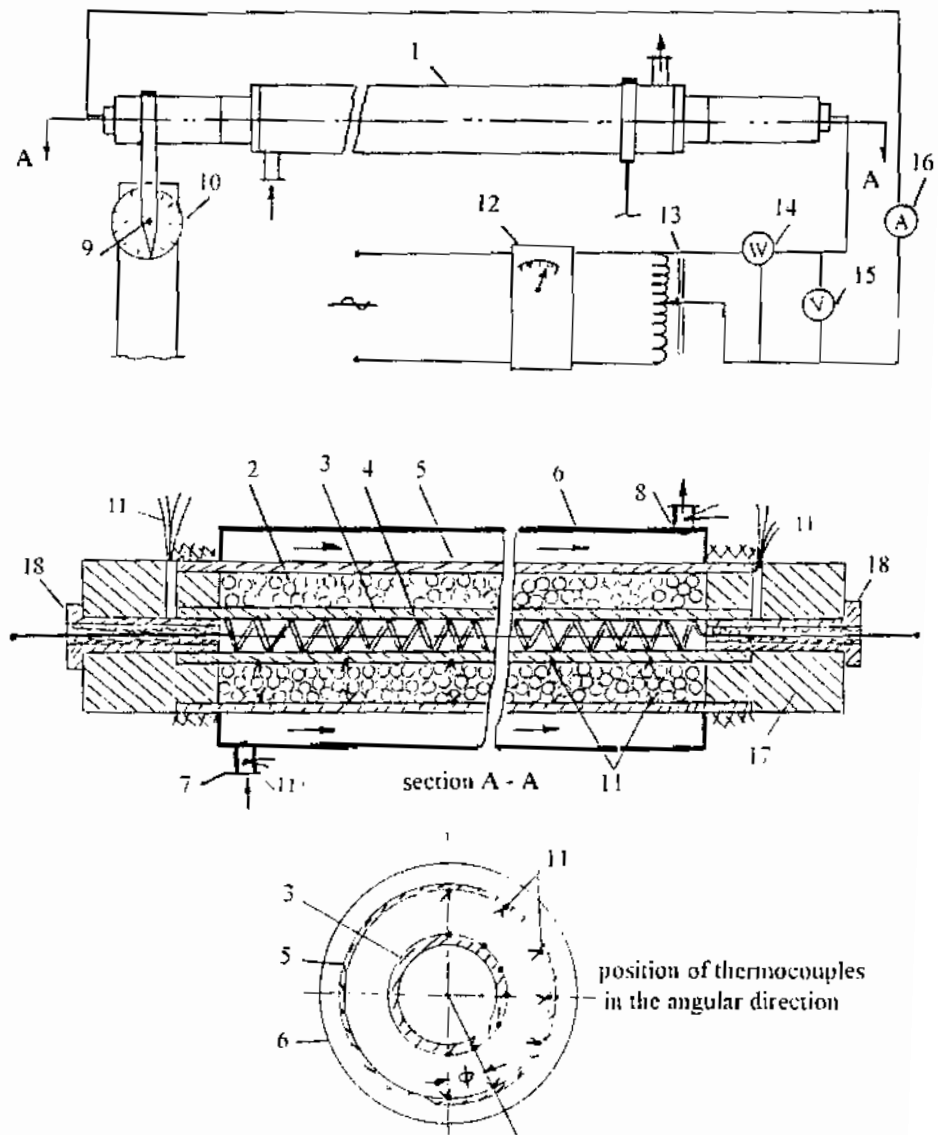


Fig. 1 Schematic layout of the experimental test apparatus

(1) annular section, (2) stainless steel spherical beads, (3) inner cylinder, (4) electric heater, (5) outer cylinder, (6) PVC cylinder, (7) bottom tap, (8) upper tap, (9) pivot, (10) protractor, (11) copper-constantan thermocouples, (12) voltage regulator, (13) variable voltage auto-transformer, (14) Wattmeter, (15) voltmeter, (16) ammeter, (17) thermal insulation, (18) teflon pins.

characteristics. The investigated parameters are: $Pr=0.7$, input heat flux at the inner wall was changed from 0.77 to 11.16 kW/m^2 with $10 \leq Ra \leq 550$, for bead diameter 6.35 mm , porosity $\epsilon=0.45$ and $Da=4.583 \times 10^{-4}$. The boundary conditions are constant heat flux on the inner wall and constant temperature at the outer one. The inclination angle was varied from the horizontal to the vertical positions with $0 \leq \theta \leq 90^\circ$.

Temperature distribution :

Figure (2) shows the temperature distribution on the inner cylinder surface in the longitudinal direction at different inclination angles ranging from $0 \leq \theta \leq 90^\circ$, and $25 \leq Q \leq 324 \text{ W}$ while Fig.(3) shows the influence of inclination angle θ on the temperature distribution t_i in the longitudinal direction for $Q = 225 \text{ W}$. A temperature drop at both ends of the inner cylinder is observed due to the end conduction losses. For the horizontal annulus, the temperature along the inner wall tends to be constant due to the equivalence of the buoyancy driven force. For non-horizontal annulus, the buoyancy driven force differs along the longitudinal line. At low inclination angles 15° , 30° and low input power 25 and 49 W , no sensible change in t_i is seen and it is nearly constant. With the increase of power, t_i increases as x increases. The increase of t_i can be classified into two portions. The lower half of the length in which the increase of t_i is relatively slow and the upper half of the rod in which t_i increases with higher rates due to the increase of buoyancy force. For $Q \geq 81 \text{ W}$, as the inclination angle increases, a drop in the temperature with negative temperature gradient in the midsection is observed and followed by positive temperature gradient. The drop in t_i is exhibited by more than one thermocouple reading. This indicates that the discussed phenomenon is not caused by some manufacturing defects. This phenomenon was achieved also by Prasad et al [14] for vertical porous annulus with constant heat flux on the inner wall with aspect ratio up to 14.4 . They admitted that there is nothing available in the literature, which can support this behavior of the recorded temperature. Their experimental data were not sufficient to provide any quantitative conclusions regarding this behavior. They concluded that it was a result of the combined effects of the solid – fluid combination, the curvature of the inner wall, and the high porosity and permeability near the wall. In the present work, where $A = 41$, this behavior is significant and can be explained by the existence of two cells of flow inside the annulus.

Figure 4 presents the temperature distribution on the inner wall along the angular direction at different inclination angles, $X/L=0.5$ and $25 \leq Q \leq 324 \text{ W}$ while Fig. 5 shows the effect of inclination angle on the inner wall temperature distribution in the angular direction for input power $Q=324 \text{ W}$. For vertical annulus, t_i is constant due to the similarity of the buoyancy force. For non-vertical annulus, with the decrease of θ , t_i decreases at the lower part and increases at the higher part causing two zones, low temperature zone in which $t_i \leq t_i$ for $\theta = 90^\circ$ and high temperature zone in which $t_i \geq t_i$ for $\theta = 90^\circ$. It increases sharply and decreases again from $\phi=120^\circ$ to 180° making a peak at $\phi=150^\circ$ indicating that the separation may occur near $\phi=150$. The peak temperature increases from 145 to 180 with the decrease of θ from 90 to 0° respectively. The length of the low temperature region increases as inclination angle

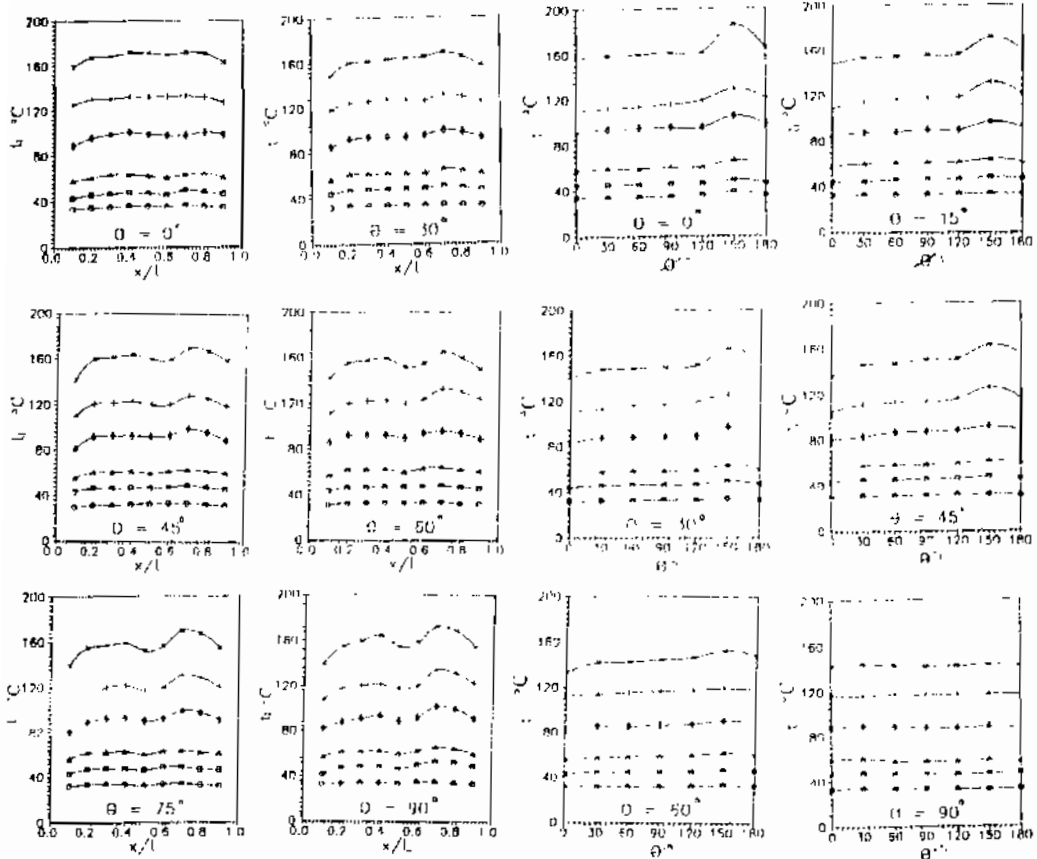


Fig. 2 temperature distribution on the inner wall in the longitudinal direction
 ○○○○○ Q=25W +++++ Q=81W - - - - - Q=225W
 □□□□□ Q=40W ●●●●● Q=144W * * * * * Q=324W

Fig. 4 temperature distribution on the inner wall along the angular direction cut
 ○○○○○ Q=25W +++++ Q=81W - - - - - Q=225W
 □□□□□ Q=40W ●●●●● Q=144W * * * * * Q=324W

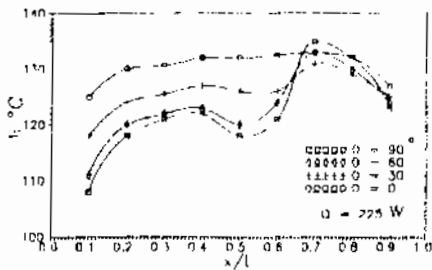


Fig. 3 influence of inclination angle θ on the temperature distribution in the longitudinal direction for $Q = 225W$

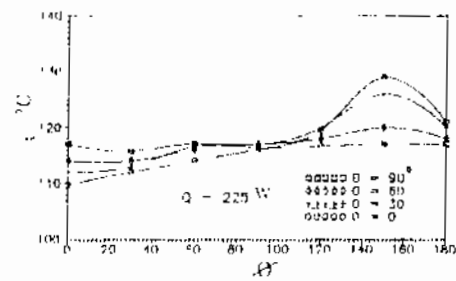


Fig. 5 effect of inclination angle on the temperature distribution in the angular direction for input power $Q = 324W$

θ increases and the length of the high temperature region decreases as θ increases.

The variation of mean temperature of the inner wall with input power is shown in Fig. 6 at inclination angles 0, 45 and 90°. The conduction solution is represented at the same graph to show the effect of convection on the inner wall temperature. With the increase of θ , \bar{t}_i decreases indicating the increase of convection part of heat transfer.

Figure 7 presents the maximum inner wall temperature, $t_{i,max}$, versus input power at different inclination angles. $t_{i,max}$ is higher for lower inclination angle. It occurs at $x/L=0.7$, $\phi=90^\circ$ for all inclination angles except at the horizontal case where $\theta=0^\circ$ in which $t_{i,max}$ occurs at $x/L=0.5$ and $\phi=150^\circ$.

Heat transfer

The effect of inclination angle on heat transfer coefficient, local and mean Nusselt number, are presented to express the heat transfer process. The variation of heat transfer coefficient with input power Q is presented in Fig. 8 at different inclination angles $\theta = 0, 30, 60$ and 90° . For low input power, $Q=4, 6W$, only conduction heat transfer exists where the heat transfer coefficient by conduction $h_c=58$. The coefficient of heat transfer increases with the increase of Q . At $\theta = 60^\circ$, with the increase of Q from 200 to 300W, h increases from 73 to 79. The heat transfer coefficient h increases also with the increase of inclination angle θ . For $Q=324W$, as θ increases from 0 to 90° , h increases from 73.6 to 84.6 kW/m²K. In order to show the behavior of the convective part of the heat transfer due to the influence of inclination angle, Fig. 9 shows the variation of the ratio h/h_c versus input power Q . This ratio starts by 1 at very low input power 4W where the conduction heat transfer only exists. The values of $h/h_c > 1$ present the convection part of heat transfer, which increases with the increase of Q and with the increase of θ . For $Q=324W$, as θ increases from 0 to 90° , h/h_c increases from 1.24 to 1.44.

The behavior of the local Nusselt number for the longitudinal direction is shown in Fig. 10 for $Q=49$ and 225W, at $\theta = 0, 30, 60$ and 90° and in Fig. 11 for $Q=225W$. For the horizontal annulus, Nu is nearly constant. For the non-horizontal annulus, at low input power $Q=49W$, Nu is nearly constant due to the very low convection. While for $Q=225W$, the effect of convection increases and the probability of existence of two cells is appeared especially for higher inclination angles, i.e., at $\theta = 60$ and 90° .

The distribution of Nu on the inner wall along the angular direction is presented in Fig. 12 for $\theta = 0, 30, 60$ and 90° at $X/L=0.5$, $Q=49$ and 225W and in Fig. 13 for $Q=225W$. For the vertical annulus, Nu is nearly constant. For non-vertical annulus, Nu decreases with the increase of ϕ due to buoyancy driven flow through porous medium. A minimum value of Nu distribution curve was observed at $\phi=150^\circ$ leading to the result, that a separation point may exist near $\phi=150^\circ$.

The behavior of \bar{Nu} with Rayleigh number, for different inclination angles is shown in Fig. 14. \bar{Nu} takes nearly constant value for $Ra \leq 40$ that is the conduction regime where $\bar{Nu}_c = (R-1)/\ln R$ [14]. For $Ra > 40$, \bar{Nu} increases as Ra increases

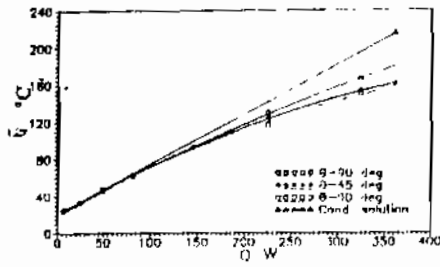


Fig. 6 variation of mean temperature with input power at $\theta = 0, 45$ and 90°

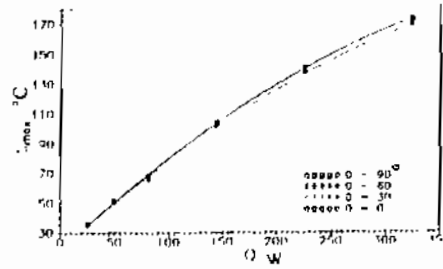


Fig. 7 maximum inner wall temperature versus input power .

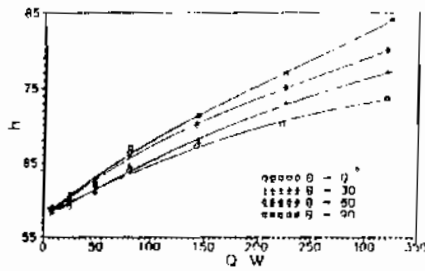


Fig. 8 variation of heat transfer coefficient with input power at $\theta = 0, 30, 60$ and 90°

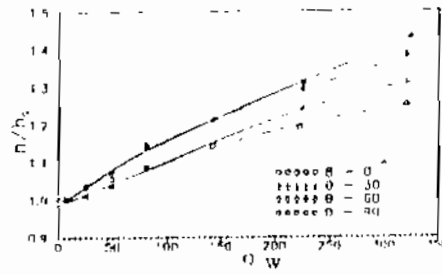


Fig. 9 variation of the ratio h/h_0 versus input power Q at $\theta = 0, 30, 60$ and 90°

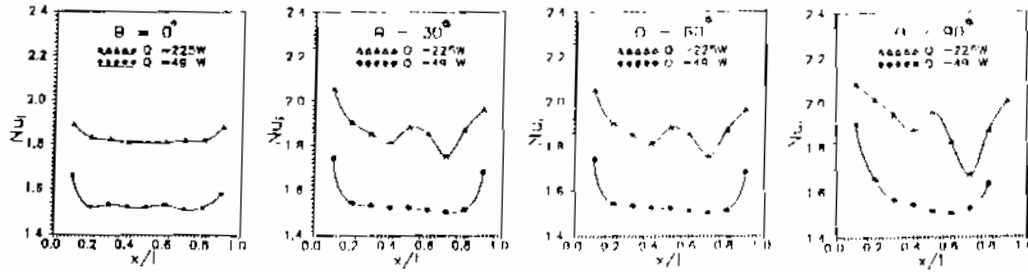


Fig. 10. local Nusselt number at the longitudinal direction for $Q=10$ and 225 W

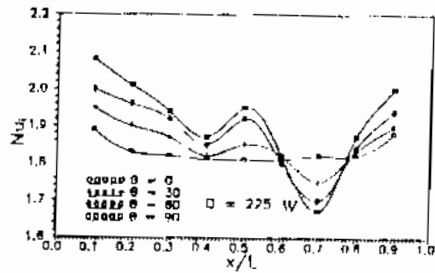


Fig. 11. local Nusselt number on the inner wall for the longitudinal direction, at $\theta = 0, 30, 60$ and 90° for $Q=225$ W .

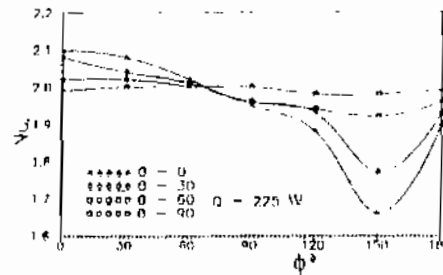


Fig. 12 local Nusselt number on the inner wall along the angular direction for $\theta = 0, 30, 60$ and 90° for $Q=225$ W .

expressing the existence of convective heat transfer. Also, \bar{Nu} increases slightly as θ increases due to the increase of buoyancy height and space in which the fluid can move. Takata et al. [18] could not catch this increase because of the low aspect ratio $A=7$, and low porosity $\epsilon=0.39$ of their studied case. The average Nusselt number is correlated with both the inclination angle θ and the Rayleigh number as follows:

$$\bar{Nu} = 1.489 e^{(3.88+2.5 \sin\theta)} 10^{-4} Ra$$

\bar{Nu}/\bar{Nu}_c is shown in Fig. 15 versus Ra . \bar{Nu}/\bar{Nu}_c is nearly equal one up to $Ra=40$. For $Re>40$ convective heat transfer causes \bar{Nu}/\bar{Nu}_c to increase as Ra increases. For $\theta=90^\circ$, as Ra increases from 100 to 550, \bar{Nu}/\bar{Nu}_c increases from 1.05 to 1.45. \bar{Nu}/\bar{Nu}_c increases also with the increase of inclination angles. For $Q = 324W$ as the inclination angle θ increases from 0 to 90° , \bar{Nu}/\bar{Nu}_c increase from 1.25 to 1.44.

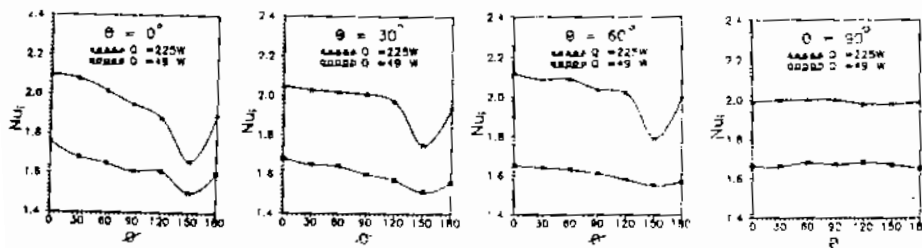


Fig. 13. distribution of Nu on the inner wall along the angular direction for $\theta = 0, 30, 60$ and 90 for $Q=49$ and $225W$.

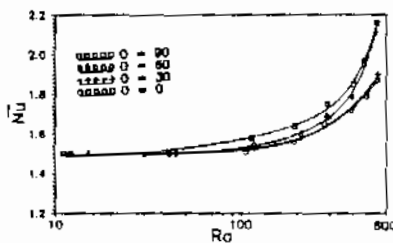


Fig. 14. behavior of \bar{Nu} with Rayleigh number for different inclination angles.

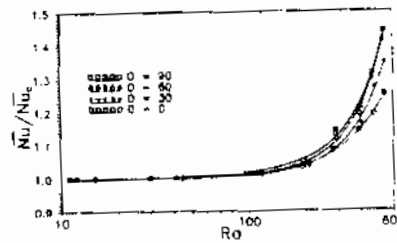


Fig. 15. behavior of \bar{Nu}/\bar{Nu}_c with Rayleigh number for different inclination angles

CONCLUSIONS

Natural convective heat transfer had been experimentally investigated in an inclined annular porous medium with height to gap ratio of 4:1 and radius ratio of 2.143 filled with stainless beads of diameter 6.35 mm, porosity $\epsilon = 0.4$ and $Da = 4.583 \times 10^{-4}$ saturated with air of $Pr = 0.7$. The inner cylinder was exposed to constant heat flux from 0.77 to 11.16 kW/m^2 with $10 \leq Ra \leq 550$ while the outer one was maintained at constant temperature. It is concluded that:

For non-horizontal annulus, t_i increases as x increases, with lower rates at the lower half of the length and with higher rates due to the increase of buoyancy force at the upper half of the rod. For high inclination angles, and high powers $Q \geq 81$, a drop

followed by an increase in the local temperature and an increase followed by a drop in the Local Nusselt number are observed near the midsection, indicating the existence of two cells of flow inside the annulus.

For non-vertical annulus, with the decrease of inclination angle, t_i in the peripheral direction decreases with an increase of Nu at the lower half and t_i increases with a decrease of Nu at the upper half. A peak temperature with a minimum value of Nu occur at $\phi=150$, indicating flow separation near $\phi=150$. The peak temperature decreases with the increase of inclination angle θ and vanishes at $\theta=90$.

With the increase of inclination angle θ , the inner cylinder mean temperature \bar{t}_i and maximum temperature $t_{i\max}$ decrease indicating the increase of convection part of heat transfer.

The conduction regime occurs for $Ra \leq 40$. For $Ra > 40$, both \bar{Nu} and \bar{Nu}/\bar{Nu}_c and the coefficient of heat transfer increase as Ra increases expressing the existence and increase of convective heat transfer. Also, the coefficient of heat transfer and both \bar{Nu} and \bar{Nu}/\bar{Nu}_c increase with the increase of the inclination angle θ . The average Nusselt number is correlated with both the inclination angle θ and the Rayleigh number as follows: $\bar{Nu} = 1.489 e^{(3.88+2.5 \sin\theta)} 10^{-4} Ra$

NOMENCLATURES

A	aspect ratio = L/δ	q	heat flux, W/m^2
c	specific heat of fluid, J/kgK	Q	input power, W
d	diameter of bead balls, m	r_i, r_o	inner and outer cylinder radii
Da	Darcy number, K/δ^2	R	radius ratio r_o/r_i
g	gravity acceleration, m/s^2	Ra	Rayleigh number
h	heat transfer coefficient, W/m^2K	t, T	temperature C, K
h_c	conduction part of heat transfer coefficient, W/m^2K	x	longitudinal length, m
k_{in}	effective thermal conductivity, W/mK	β	thermal expansion coefficient, K^{-1}
K	permeability of porous medium, m^2	ν	kinematic viscosity of fluid, m^2/s
L	effective length of test section, m	ρ	density of fluid, m^3/kg
Nu	local Nusselt number	ϵ	Porosity
Nu	mean Nusselt number	δ	gap width = $(r_o - r_i)$, m
Pr	Prandtl number	θ	Inclination angle
		ϕ	angular inclination angle

REFERENCES

1. Facas, G. and Farouk, B., "Transient and steady state natural convection in a porous medium between two concentric cylinders" ASME Journal of Heat Transfer, Vol. 105, pp. 660-663, 1983.
2. Vasseur, P., Nguyen, T., Robillard, L., and Tongthi, V., "Natural convection between horizontal concentric cylinders filled with a porous layer with internal heat generation", Int. J. Heat and mass transfer, Vol. 27, pp.337-349, 1984.

3. Raw, Y., Fukuda, K., and Hasegawa, S., "Steady and transient analysis of natural convection in a horizontal porous annulus with Galerkin method" ASME Journal of Heat Transfer, Vol.109, pp. 919-927, 1987.
4. Raw, Y., Fukuda, K., and Hasegawa, S., "A numerical study of 3-D natural convection in a horizontal porous annulus with Galerkin method", Int. J. Heat and mass transfer, Vol. 31, pp. 695-707, 1988.
5. Himasekhtar, K., and Bau, H., "2-D bifurcation phenomena in thermal convection in horizontal, concentric annuli containing saturated porous media", J. Fluid Mechanics, Vol. 187, pp. 267-300, 1988.
6. Mojtabi, A., Mojtabi, M., Azaiem, and Labrosse, G., "Numerical and experimental study of multi cellular free convection flows in an annular porous layer", Int. J. Heat and Mass transfer, Vol. 34, pp. 3061-3074, 1991.
7. Mojtabi, A, and Mojtabi, M., "Analytical solution of steady natural convection in an annular porous medium evaluated with a symbolic algebra code" ASME Journal of Heat Transfer, Vol.114, pp.1065-1067, 1992.
8. Barbosa, J., and Saadjiou, A., "Natural convection in a porous, horizontal, cylindrical annulus" ASME J. of Heat Transfer, Vol. 116, pp. 621-626, 1994.
9. Mojtabi, A., "Numerical simulation of 2-D and 3-D free convection flows in a horizontal porous annulus using a pressure and temperature formulation," Int. J. Heat and Mass transfer, Vol. 40, pp. 1521-1533, 1997.
10. Reda, D.C., "Natural convection experiments in a liquid saturated porous medium bounded by vertical coaxial cylinders" ASME Journal of Heat Transfer, Vol.105, pp. 795-802, 1983.
11. Prasad, V. and Kulaki, F., "Natural convection in a vertical porous annulus," Int. J. Heat and Mass transfer, Vol. 27, pp. 207-219, 1984.
12. Prasad, V. and Kulaki, F., "Natural convection in porous media bounded by short concentric vertical cylinders," ASME Journal of Heat Transfer, Vol.107, pp.147-154, 1985.
13. Prasad, V, Kulaki, F., and Keyhani, M., "Natural convection in porous media" J. Fluid Mech., Vol.150, pp. 89-119, 1985.
14. Prasad, V., Kulaki, F., and Kulkarni, A., "Free convection in a vertical porous annulus with constant heat flux on the inner wall-experimental results", Int. J. Heat and Mass transfer, Vol. 29, pp. 713-723, 1986.
15. Prasad, V., "Numerical study of natural convection in a vertical porous annulus with constant heat flux on the inner wall," Int. J. Heat and Mass transfer, Vol. 29, pp. 841-853, 1986.
16. Fukuda, K., Takata, Y., Hasegawa, S., Shimomura, H. and Sanokawa, K., "3-D natural convection in a porous medium between concentric inclined cylinders," Proc. 19th National Heat Transfer Conf., Vol. HTD-8, pp. 97-103, 1981.
17. Takata, Y., Fukuda, K. and Hasegawa, S., "Experimental study on natural convective heat transfer in a porous medium enclosed in an inclined cylindrical annulus," Tech. Report of Kyushu University, No. 83-0101, pp. 832-838, 1983.
18. Takata, Y., Fukuda, K., Hasegawa, S., Iwashige, K., Shimomura, H., and Sanokawa, K., "Three-dimensional natural convection in a porous medium enclosed with concentric inclined cylinders," Japan Atomic Energy Research Institute, NC41, pp. 351-356.